NATIONAL ADVISORY COMMITTEE FOR AERONAUTICS

TECHNICAL NOTE 3933

EFFECT OF FIBER ORIENTATION ON BALL FAILURES
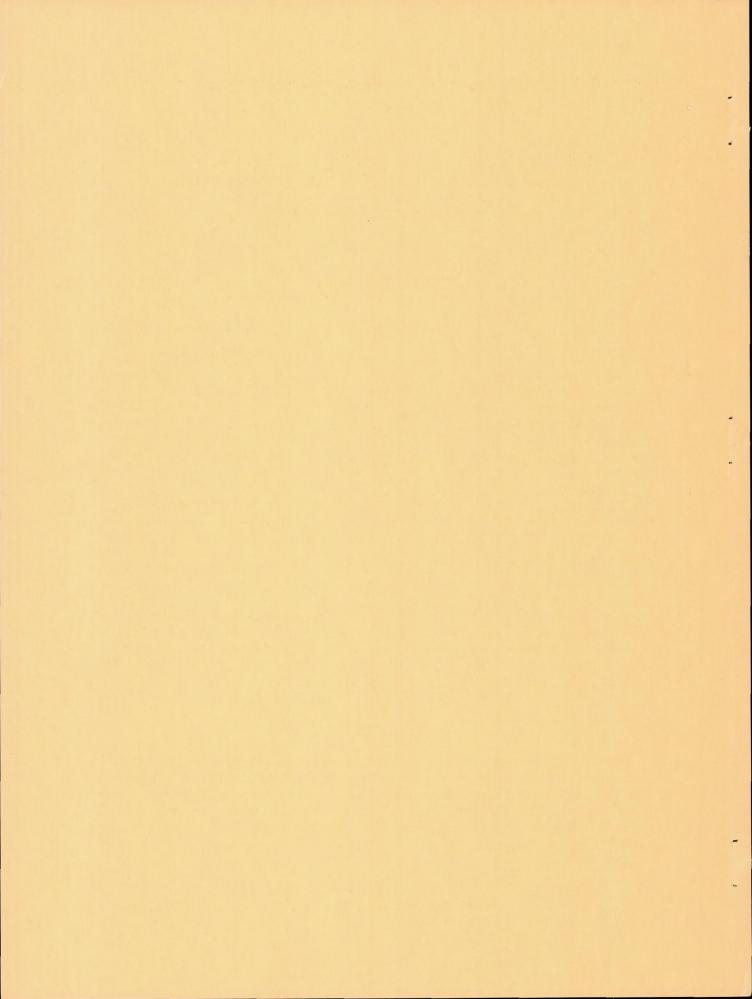
UNDER ROLLING-CONTACT CONDITIONS

By Robert H. Butler, H. Robert Bear, and Thomas L. Carter

Lewis Flight Propulsion Laboratory
Cleveland, Ohio

NACA

Washington

February 1957

NATIONAL ADVISORY COMMITTEE FOR AERONAUTICS

TECHNICAL NOTE 3933

EFFECT OF FIBER ORIENTATION ON BALL FAILURES UNDER

ROLLING-CONTACT CONDITIONS

By Robert H. Butler, H. Robert Bear,

and Thomas L. Carter

SUMMARY

Two series of rolling-contact fatigue tests were conducted in a bench-type rig developed at the NACA Lewis laboratory. In one series 1/2-inch balls made of SAE 52100 and AISI M-1 steel were tested at an ambient temperature of 80° F and at maximum Hertz stresses up to 720,000 pounds per square inch. The effect of fiber orientation was observed with the ball track restricted to passing directly over the poles or coincident with the equator. These tests were conducted using a synthetic lubricant.

To obtain additional evidence 29 failed balls from tests of 150 balls conducted to determine the stress-life relation of the rig were macroetched to determine failure location. These 9/16-inch balls were tested at stresses of 600,000 to 750,000 psi at room temperature using a mineral oil lubricant. Parallel flats 3/16 inch in diameter were ground on each ball to assure random track orientation.

Analysis of failure position showed that approximately twice as many failures occurred in the polar areas as would be expected if the ball were of uniform fatigue strength over the entire surface. Most early failures resulted from polar weakness (open end grain), large inclusions, or macroscopic corrosion spots.

INTRODUCTION

The problem of developing satisfactory high-temperature rolling-contact bearing alloys (at present these are primarily steels) is complicated by lack of rolling-contact fatigue data on these alloys. A survey of the information available and of the problem is given in reference 1. Additional background on the need for new steels may be found in references 2 to 5.

Carrying out a program of developing new steels with superior rolling-contact fatigue properties will require extensive investigation into the many factors involved. One factor is the degree and type of forging performed upon the material during the manufacture of bearing parts. Steel balls as manufactured for bearings are made by upsetting slugs of steel rod between hemispherical dies. The resulting rough ball is then heat-treated and rough and finish ground. This type of forging produces a pronounced fiber orientation which results in a ball having two end grain (polar) areas which etch preferentially. The purpose of this study was to determine the effect of fiber orientation on ball failure position and ball life.

Factors significant in ball life can be isolated more readily when the variables involved are controlled. The rolling-contact fatigue spin rig offers an opportunity for this type of controlled experiment. This investigation is an analysis of the position of ball failure with respect to fiber orientation. A limited analysis of the effect of fiber orientation on ball life is also given.

The balls were tested with ball track orientation (1) over the end grain (pole), (2) coincident with the equator, and (3) at random.

APPARATUS

To simplify the presentation of results only brief descriptions of the apparatus and procedure are presented here. Details are given in appendix A. Figure 1(a) is a cutaway view of the rolling-contact fatigue spin rig. The test specimens were two test balls revolving in a plane on the bore of the test cylinder (fig. 1(b)). Air at pressures up to 100 pounds per square inch was introduced through the nozzles to drive the balls at high orbital speeds. The loading on the balls was that produced by centrifugal force, and the stress was calculated according to the methods of reference 6. Approximately 5 milliliters per hour of lubricant were introduced in droplet form into the drive airstream between the guide plates.

Orbital speed was measured by counting the pulses from a photo-amplifier on an electronic tachometer. A ball or race failure resulted in the generation of a large signal from a velocity pickup attached to the rig. This signal when amplified actuated a meter relay which shut down the system.

The steels used for the balls were SAE 52100 and AISI M-1. Cylinder steels were AISI M-1 and AISI M-50 (MV-1). Table I lists the compositions of these steels. Cylinders were 4.750 inches in outside diameter and 3.00 inches long, and the bore diameters ranged from 3.250 to 3.550 inches. The test balls were nominally 1/2 and 9/16 inch in diameter.

PROCEDURE

Before the test all cylinders were given dimensional surface finish and hardness inspections, and all test balls were weighed and given an examination at a magnification of 60. Prior to inspection and use, test specimens were flushed and scrubbed with 100 percent ethyl alcohol and clean cheesecloth. Care was taken during assembly not to scratch the bore surface. The bore surface and test balls were coated with lubricant during assembly.

The rig was brought up to operating speed as rapidly and smoothly as possible. Speed, air pressure, and vibration levels were recorded during the test. Table II outlines the test conditions for both sizes of balls tested. After post-test examination all balls were macroetched to locate positions of failures and to measure track orientation. Post-test examination consisted of examining the failed balls at a magnification of 60 before macroetching to determine whether surface factors were responsible for the failure. All failures were photographed for record purposes. Because of the need for many data photographs, a setup for photographing ball surfaces was developed. The details are given in appendix A.

RESULTS AND DISCUSSION

The primary information obtained was the position of failure with respect to fiber orientation of the ball. The studies were based on 1/2-inch-diameter balls with modified geometry so that they were run either over the poles or on the equator. The studies also gave some limited life data which are reported.

To supplement these results, 9/16-inch-diameter balls were etched and their failure positions noted. These results are herein reported, and they support the results of 1/2-inch-ball studies.

Fiber Orientation

Effect of failure location. - The tests considered in this report were run with the track oriented over the polar areas, coincident with the equator, or randomly selected. If a test ball were of uniform fatigue strength over its entire surface area, the number of failures in any area would be proportional to the ratio of the track length through the area to the total track length. For randomly selected track orientations, a large sample was assumed, and average values were calculated for the track lengths passing through the polar areas. By assuming a material of uniform fatigue strength, one can calculate the theoretical distribution of failures in any given area of the ball surface under a given set

of track orientation restrictions for a homogeneous material. These cal-
culations are summarized in appendix B. By comparing the distribution
of failures actually occurring in a given area with the distribution
theoretically predicted for a homogeneous material, one can determine the
extent to which a characteristic area of the ball surface deviates from
the average fatigue strength of the ball.

Table III is a summary of results for 13 1/2-inch SAE 52100 balls.
Each ball had a hole drilled in the plane of the equator so that
the track passed directly over the poles (at an angle of 90° to the
equator). Of these balls, all but one (92%) failed in the polar area,
although the portion of the track within the polar areas (the probability
of failure in the polar area for a homogeneous material) was only about
42 percent of the total track length. The portion of the polar failures
was more than twice as great as that which would be expected if the polar
areas were of the same fatigue strength as the remainder of the ball.

Twenty-one 1/2-inch SAE 52100 balls were tested with holes drilled
perpendicular to the plane of the equator so that the track was coinci-
dent with the equator. Since the track was entirely within one charac-
teristic surface area, no direct comparison could be made with the polar
areas. However, as shown in figure 2, most of these balls (16 out of 21)
were unfailed after the number of cycles during which all of the balls
running over the poles had failed.

A further source for comparison of the strength of polar and non-
polar areas of a ball was provided by a group of 9/16-inch-diameter
SAE 52100 balls. These balls were not as a group restricted to one pre-
ferred track location, thus each ball had a fixed track randomly selected.
A simple check of this random orientation was made by calculating (appen-
dix B) the portion of the tracks that passed through the poles. The
results were compared with the actual results to confirm random track
orientation.

Balls were etched to expose polar and equatorial areas. Balls with
a track clearly within the polar area or not entering a polar area were
so classified. Because of a finite track width and a somewhat indefinite
polar boundary, some tracks could not be clearly classified and were
placed in a separate category. For comparison purposes with theoretical
calculations of track orientation it is assumed that this boundary group
is divided evenly between polar and nonpolar tracks. This is justified
by the fact that the maximum shear stress, which is the most critical
stress, lies under the center of the track and is equally likely to fall
within or without the polar area when the track is split by the pole
boundary. Table IV is a comparison between the actual track locations
for 150 balls and the theoretical distribution calculated in appendix B.
It can be seen that the theoretical and actual results are very close,
and the tracks can be considered randomly oriented.

4271

      Since the tracks of the 150 balls were randomly oriented with respect
to characteristic areas of ball geometry, a random failure pattern should
have been produced if the balls were of uniform fatigue strength over the
entire surface area. Appendix B contains a computation of the probability
of a failure occurring in a polar area under various limiting conditions.
Table V is a comparison of the actual failure locations with the results
anticipated from the theoretical results of appendix B. The proportion
of polar failures is approximately twice that to be expected from a
homogeneous surface. This strong susceptibility of polar areas to failure
indicates that the polar areas are significantly weaker in fatigue.

      Table VI gives the distribution of failures in the 16 balls out of
the 29 in table V that ran over the poles (not including polar boundary
tracks). If the balls were of uniform fatigue strength, the portion of
failures occurring in the poles would be proportional to the average
track length occurring within the poles (23.4 percent, appendix B). The
actual result (44 percent) was almost twice that number.

      Figure 3 is a plot of failure density as a function of ball latitude
for the 29 failures obtained in the stress-life tests. The data were
plotted by orienting all failures along a given longitude and dividing
the number of failures in a zone between two latitudes by the ratio of
the zone area to the hemispherical area. This plot shows a very marked
increase in the density of failures at higher ball latitudes, that is,
in polar areas. Such a plot for a homogeneous material would produce
a circular band.

      Tables III, V, and VI show that the SAE 52100 balls tested under
rolling-contact stresses show a significant preference for polar area
failures over that to be expected if the ball surface is of uniform
fatigue strength.

      Since the primary characteristic which distinguishes the polar area
from the remaining portion of the ball is the orientation of the fiber
perpendicular to the surface (fig. 4(a)), one might expect the equator
area, which often has a similar grain flow, to be weak in fatigue also.
This equator end grain results from the removal of the flashing formed
during upsetting of the ball. This condition can be seen in figure 4(b)
and to some extent in figure 4(a). Only one failure was directly on the
equator, but no distinguishing appearance of any significance was noted.
This series of tests does not show any conclusive evidence of equator
weakness or strength. However, a large portion of the nonpolar failures
have, from surface examination, some pronounced imperfections which have
a consistent orientation to the equator. Of the 18 balls failing other
than at the equator or in a polar area, nine had a crack or open inclusion
perpendicular to the ball equator and passing through or collinear with a
fault line in the fatigue pit. Examples of this condition are shown in
figure 5. Of the remaining nine failures, one was at the location of a

large corrosion pit detected in the prerun inspection, and three were on
balls having fine corrosion detected before running. The remaining five
balls had no cause of failure apparent to surface examination. Metallog-
raphic investigation is planned as a followup to these tests.

Effect on life. - Fiber orientation also had an effect on life of
SAE 52100 balls tested at room temperature. Figure 6 is a Weibull plot
of the lives of the balls running over the poles. The ordinate is the
log log of the reciprocal of the fraction of the test balls surviving for
a given life, and the abcissa is the log of life in millions of stress
cycles. This method of data presentation is standard for bearing fatigue
failures; however, a brief outline of the procedure is given in appendix
C. The 10 percent life is interpolated from the curve and is equal to
17.5 million cycles for this group of balls.

Equivalent data for the SAE 52100 balls run on the equator tested
at room temperature cannot be given because of the few failures obtained.
A comparison of the scatter in lives between the polar failures and the
equator failures is shown in figure 2. The results, except for the three
quick failures (fig. 2(b)), indicate that the 10 percent life for these
balls could be many times greater than that for the pole failures. The
resulting life of the cracked ball indicates that the other early failures
may have been caused by similar defects that were hidden.

The results obtained from the 29 failed balls out of 150 run in the
stress-life tests also show a tendency for pole failures and failures due
to forging defects to occur at shorter lives than other failures.

Table VII is a summary of failure cause and location with the balls
in order of increasing life. For ease of comparison, all lives were con-
verted to the 675,000 psi level. It can be seen that failures originating
in the poles and through surface defects perpendicular to the equator
tend toward the shorter life end of the table. The nonpolar failures
with no obvious surface defects tend to have longer lives.

The results of the AISI M-1 equator tests are also plotted in figure
2(c). These results indicate a trend similar to that of the SAE 52100
equator results. This steel was dirtier than the SAE 52100 steel. Slag
streaks such as the ones shown in figure 7(a) were found on about one
out of every three balls examined at a magnification of 60. These slag
streaks undoubtedly contributed to the short lives of these balls.
Several failures occurred at these defects. Figure 7(b) illustrates
this effect.

Effect on life scatter. - The slope of the Weibull line for the pole
failures of the 1/2-inch balls (fig. 6) is a measure of the dispersion
of the life data. The slope of the line compares favorably with the
accepted value given for rolling-contact bearings (10/9) in reference 7.

Macroscopic Observations

Surface damage such as scratches was not found to be harmful. Slag streaks and large inclusions were damaging because they extended into the ball some distance.

All failures observed were similar in appearance, and the extent of spalling ranged as shown in figure 8(a) and (b) (ref. 8). The spalls were similar to those encountered in full-scale bearing failures. Polar failures are the same in appearance as other failures; figure 9 is a macroetched section through a typical pole failure.

Microscopic Observations

The detailed observations in reference 8 show that structural non-homogeniety (chemical segregation) and matrix cracking caused by small inclusions were contributory to failure. Undoubtedly these factors were important in the longer life failures.

SUMMARY OF RESULTS

Rolling-contact fatigue studies were made using the rolling-contact fatigue spin rig on 1/2-inch-diameter balls of SAE 52100 and AISI M-1 steel and on 9/16-inch-diameter balls of SAE 52100 steel at an ambient temperature of 80° F and at maximum Hertz stresses up to 750,000 psi. The results of these studies are as follows:

1. The area of an SAE 52100 ball that is weak in fatigue is the polar area where the fiber orientation is generally perpendicular to the surface. Fiber orientation strongly influenced both the position of failures and the number of stress cycles to failure for the 1/2-inch SAE 52100 balls. Of the balls run over the poles, 92 percent failed within a polar area. The theoretical probability of failure is 42 percent in this area. The balls run over the equator had lives (10 percent failures) many times greater than the balls over the poles.

2. Further evidence of polar-area weakness in fatigue was obtained from an analysis of balls tested with random track orientation. The percentage of ball fatigue failures occurring in the polar areas was about twice that to be expected from a ball whose surface area is of uniform fatigue strength. Thus there appears to be a significant weakness in fatigue at the open end grain polar areas of balls used in rolling-contact bearings.

3. A large portion of the nonpolar failures appear to be caused by surface defects bearing a relation to forging lines emanating from the formation of the ball from rod stock. This condition and the polar end grain explain most of the early ball failures produced in the tests.

Lewis Flight Propulsion Laboratory
    National Advisory Committee for Aeronautics
        Cleveland, Ohio, December 17, 1956

APPENDIX A

APPARATUS AND PROCEDURE

Test Rig

As is previously stated, figure 1(a) is a cutaway view of the rolling-contact fatigue spin rig. The test specimens are the two test balls revolving in a plane on the bore of the test cylinder (fig. 1(b)). Air at pressures to 100 psi is introduced through the nozzles to drive the balls at high orbital speeds. The nozzle system and the cylinder are held together by upper and lower cover plates fastened by three removable bolts. The rig assembly is supported from a rigid frame by three flexible cables. In order to keep external constraint at a low value, the drive air is introduced into the rig through a 6-foot-long flexible metal hose.

Operation. - The two test balls separate and maintain relative positions 180° apart at orbital speeds above the critical frequency. A detailed analysis of the rig operation may be found in reference 9.

Loading. - The only loading on the balls is that produced by centrifugal force, and it is in excess of 700 pounds for a 1/2-inch ball revolving in a 3.25-inch-bore test cylinder at an orbital speed of 30,000 rpm. At this speed a maximum Hertz stress of approximately 750,000 psi will be developed in the center of contact.

Lubrication. - Lubrication is accomplished by introducing droplets of the lubricant into the drive airstream between the guide plates (fig. 1(a)). The rotating airstream forces the droplets against the bore of the test cylinder.

Lubricant flow rate is controlled by regulating the pressure upstream of a long capillary tube. The pressure drop through the capillary was sufficient to give excellent control of the flow for small flow rates. The lubricant flow rate used in both series of tests was approximately 5 milliliters per hour. The lubricant used in the 1/2-inch-ball tests was a synthetic diester (di-2-ethylhexylsebacate) which met the MIL-L-7808 specifications for aircraft turbine-engine lubricants except for the low-temperature-viscosity requirements. The lubricant used for the tests of the 9/16-inch balls was a mineral oil (SAE 10).

Instrumentation. - The two major instrumentation requirements for the rig are a speed measurement and control system and a failure detection and shutdown system.

Orbital speed is measured by counting the pulses from a photoamplifier on an electronic tachometer. The pulses are generated by the two test balls interrupting a light beam to the photocell. A magnetic pickup may also be used for measuring system speed at room temperature.

Failures are detected by comparing the amplified signal from a velocity vibration pickup (attached to the rig, see fig. 1(a)) against a predetermined signal level that is preset on a meter relay. The large vibration amplitude resulting from a ball or cylinder failure trips the meter relay and results in shutdown of the test.

Air supply. - The drive air is dried to less than 30 percent relative humidity and then filtered before being used in the rigs.

Materials

The ball materials chosen to be tested were SAE 52100 and AISI M-1. SAE 52100 is the standard steel used for precision ball and roller bearings and was chosen for reference purposes. AISI M-1 was chosen because some experience had been obtained with this steel in laboratory tests and field applications. The cylinder materials for the 9/16-inch balls were the tool steels AISI M-1 and AISI M-50 (MV-1). The nominal analyses of these steels are given in table I.

Test Specimens

Cylinders. - The dimensions of the test cylinders are as follows: outside diameter, 4.750 inches; length, 3.00 inches; initial nominal inside diameter, 3.250 inches. The bore surface finish was 2 to 3 microinches for all cylinders. Roundness of the bore was held to 0.0001 inch and bore taper to a maximum of 0.0003 inch. Hardness measurements were taken on the cylinder ends. Each cylinder was uniform within 2 hardness numbers, although average hardness varied from Rockwell C-60 to 64 for different cylinders.

Between 10 and 15 tests may be run on a bore surface. The bore is then reground 0.060 inch larger and refinished. This new surface is about 0.022 inch below the location of the maximum shear stress of the previous tests, and so the effects of prior stressing are considered to be negligible. Failure positions on one cylinder surface do not correlate with failure positions of the previous test surface.

Test balls. - By taking advantage of the fact that a rotating body free to adjust itself will rotate about the axis of maximum rotational inertia, test balls may be modified so that they will rotate about any fixed axis. The test balls of both materials were of grade 1

specifications and were hardened to Rockwell C-63 to 64. Each 0.500-inch-nominal-diameter ball had its geometry modified during manufacture by a 0.050-inch hole drilled diametrically through it. The hole was drilled either parallel or perpendicular to the forging direction. This hole established a fixed axis of rotation and caused the ball to roll either coincident with the equator or over the poles. Figures 10(a) and (b) are schematic illustrations of this modification. Figure 4(a) is a macrophotograph of an etched SAE 52100 ball showing the chemical segregation that is referred to as fiber orientation. End grain occurs at both poles and at the equator (fig. 10(b)). The 9/16-inch-diameter balls were "off the shelf" grade 1 balls. To establish a random track orientation, each ball had parallel flats 3/16 inch in diameter ground on it in a random manner.

PROCEDURE

Pretest Inspection

Cylinders were given dimensional surface finish and hardness inspections. This was followed by a magnetic particle inspection for both cracks and large subsurface inclusions and a visual inspection for deep scratches and other mechanical damage.

All test balls were weighed and given an inspection at a magnification of 60. The presence of excessive scratches or pitting, and any cracks, laminations, or flat spots was noted in a permanent record. Some of the 1/2-inch balls were given a 30-minute polish with a Gamal polishing cloth and levigated alumina. This resulted in a marked carbide relief on the AISI M-1 balls, but only removed the finer scratches on the SAE 52100 balls. This procedure exposed defects (such as fine laminations and cracks) that were previously hidden by the surface finish.

Prior to inspection and use, test specimens were flushed and scrubbed with 100 percent ethyl alcohol and clean cheesecloth. This procedure left a thin film of grease on the surface, but this was considered desirable to minimize corrosion.

Assembly of Rig

The rig and test specimens were cleaned and assembled with care to prevent scratching of the bore surface. The bore surface and test balls were coated with lubricant. The test position in the cylinder was set by loosening the collet (fig. 1(a)) and moving the nozzle assembly and the test balls axially to the test station and then retightening the collet. The rig was mounted in the support frame and then leveled. Oil and air supply lines and the vibration pickup were connected. The final step was to check the alinement of the light beam on the photocell.

Starting and Running Procedure

The rig was brought up to operating speed as rapidly and as smoothly as possible. The rig could then be switched to automatic speed control or left on manual control. On manual control the rig speed must be corrected at intervals to compensate for the speed increase due to run-in of the test specimens. Run-in is rapid for the first few hours, and it is practically complete after the first 48 hours.

Speed and oil flow were monitored regularly. Speed, air pressure, and vibration levels were recorded at each reading. The test was continued until a predetermined number of stress cycles had been exceeded or until a ball or race failure actuated the meter relay which shutdown the rig.

Stress calculations. - With ball weight, speed, and orbital radius of rotation of the test balls known, the load can be calculated. The stress developed in the contact area was calculated from the load and specimen geometry by using the modified Hertz formulas given in reference 6.

Post-Test Inspection

After tests the failed balls were examined at a magnification of 60 in order to determine whether surface-appearing factors were responsible for the failure.

Macroetching. - When it was decided not to section a ball, the ball was etched in a 50 percent hydrochloric acid solution (at 160° F) to determine the location of the failure relative to the poles. To preserve failure detail, stopoff lacquer was painted on the failure prior to etching. Etching was complete when the polar areas and the equator were clearly defined; this required about 5 minutes. The balls were then flushed with water and alcohol. After drying they were stored in a desiccated atmosphere until geometry measurements could be taken. For protection during storage the balls were dipped in a solution of paraffin in varsol to inhibit rusting. For balls that were sectioned, failure locations (polar or nonpolar) were determined after sectioning.

Photography. - The difficulty in accurately describing or sketching the many surface conditions pertinent to the analysis of ball fatigue failures and the large number of balls investigated created a need for an accurate and quick recording method. A photographic record of significant surface conditions observed during prerun and post-run ball inspections would be very helpful. The photography of a small highly polished spherical surface presented a difficult illumination problem. Any conventional method of illumination would produce an intolerable

amount of glare and high contrast between the hot spot produced by the
reflection of the light source and the remaining area within the field
of view. Figure 11 is a diagram of the photographic apparatus. A rela-
tively large piece of ground glass was placed between the specimen and
the objective lens. A hole just large enough not to interfere with the
optics of the microscope was cut in this glass. The ground glass was
illuminated by a standard light source. The ground glass presented soft
indirect illumination of the ball specimen. The reflection of this source
of illumination was greater in size than the field of view of the micro-
scope, so the entire area in view was of the same order of magnitude of
brightness. The only dark spot was the image of the small hole necessary
for viewing with the microscope. This was small enough to be placed in
some unimportant area and was not considered objectionable. A reflex
housing and a 35-mm camera were used for simultaneous viewing and
photographing.

Measurement of track orientation. - After etching, the polar areas
and the equator of the ball are clearly defined. The flats on the balls
define the track location. Rotating the balls about the flats and marking
the track with a pencil clearly defined the track. If the equator was
not clearly visible, it was marked by rotating the ball about the poles.
The ball was placed in a holder calibrated in polar coordinates, and the
equator alined with the cross hair of a low-power viewing microscope.
The holder and ball were then rotated until the track was in line with
the cross hair. The angle through which the ball holder had been rotated
was the angle of intersection of the track and equator. The smaller of
the two possible angles was taken; thus all measurements were 90° or less.
This angle is defined as α shown in figure 12.

The angle in the plane of the track between the equator-track inter-
section and the center of the failure was next measured. This was done
by alining the intersection with the microscope cross hair, rotating the
ball until the failure was alined, and measuring the angle of rotation
with a calibrated ball holder. The angle of 90° or less was always the
one recorded. This angle is defined as β shown in figure 12. The
angles α and β define the track orientation and failure location on
the ball.

With the poles clearly defined and the track indicated by a pencil
line, the location of the track relative to the polar areas could be
determined. Inspection under a low-power microscope determined whether
the track (1) passed through the pole, (2) passed through the polar
boundary, or (3) was contained entirely within nonpolar areas of the
ball surface.

APPENDIX B

DERIVATION OF THEORETICAL TRACK AND FAILURE DISTRIBUTIONS

OVER BALL SURFACE

In order to determine whether any area of the ball is weaker in fatigue than the remaining area, it is necessary to calculate the expected percentage of failures assuming uniform fatigue strength over the entire surface of the ball. First calculate the expected percentage of tracks passing through a given area. Figure 13 shows that the pole surface area lies within a cone of half-angle A cutting the surface of the sphere.

Probability of Track Passing Through Pole Area When Tracks

Are Randomly Distributed Over Ball Surface

To define the track it is only necessary to define the axis of rotration. The probability P_S that the axis will pass through any surface area is the ratio of that area to the area of the hemisphere, or

$$P_S = \frac{r^2 \cos \theta d\theta d\varphi}{2\pi r^2} \tag{1}$$

where r is the radius, θ is the hemisphere latitude, and φ is the longitude angle (fig. 13).

To get the cumulative probability that the track will pass through the poles P_{tp}, integrate both sides of equation (1). This yields

$$P_{tp} = \frac{1}{2\pi} \int_0^{2\pi} \int_0^A \cos \theta \ d\theta \ d\varphi \tag{2}$$

The axis may be contained anywhere in the zone whose height is determined by $h = r \sin A$. The orthogonal plane of the axis will still pass through the pole, so the limits on integration are $0 \leq \theta \leq A$ and $0 \leq \varphi \leq 2\pi$. Then the probability of the track passing somewhere through the pole is equal to

$$P_{tp} = \sin A \tag{3}$$

For the 9/16-inch-diameter balls P_{tp} is equal to 0.64 for $A = 40°$.

Probability of Failure in Pole When Tracks Are Randomly

Distributed Over Ball Surface

The combination of the probability of a track passing through the pole P_{tp} and the probability of failure on the pole on those tracks that pass through it P_{tf} gives the probability for pole failure with randomly located tracks. The first probability is $\sin A$. The probability that the ball will fail on a track in the pole is the ratio of the polar area to the total hemispherical area, or

$$P_{tf} = \frac{2\pi r^2 (1 - \cos A)}{2\pi r^2} = 1 - \cos A \qquad (4)$$

and the probability for pole failure with randomly oriented tracks is then

$$P_{ptf} = \sin A \,(1 - \cos A) \qquad (5)$$

which is equal to 0.15 for 9/16-inch balls with $A = 40^\circ$.

Probability of Pole Failure if Track

Passes Through Center of Pole

The probability of a pole failure if the track is constrained to pass through the center of the pole P_{ftf} is the ratio of the arc length of the track passing through the pole to the hemispherical arc length of the track:

$$P_{ftf} = \frac{2rA}{180r} = \frac{2A}{180}$$

which is equal to 0.42 for 1/2-inch balls with $A = 38^\circ$.

APPENDIX C

PRESENTATION OF BEARING FATIGUE DATA

A distribution function developed by Weibull fits the observed scatter in the fatigue lives of rolling-contact bearings (ref. 10). Because of the usually small sample (about 30 bearings) involved, the data cannot reliably be fitted into a frequency curve. Instead the cumulative form of the distribution is used. The cumulative distribution function (Weibull) is as follows:

$$\log \frac{1}{S(L)} = GL^e \tag{1}$$

where $S(L)$ is the fraction of the sample surviving the first L stress cycles, and G and e are positive constants.

Figure 6 uses special probability paper on which the Weibull distribution becomes a straight line of slope e. The ordinate represents $\log \log 1/S(L)$, but is graduated in terms of the fraction failed at L stress cycles.

A set of data is ordered according to life, and each succeeding life is given a rank (statistical percentage) and is plotted on Weibull paper. If the median rank is used, a line is drawn which takes the general direction of the array of points and which splits the array in half. A median rank is an estimate of the true rank in the population that has an equal probability of being too large or too small.

A table of median rank values for sample sizes up to 20, and formulas for calculation of the median rank values for any order position in any sample size is given in reference 10.

REFERENCES

1. Butler, Robert H., and Carter, Thomas L.: Stress-Life Relationship of the Rolling-Contact Fatigue Spin Rig. NACA TN 3930, 1957.

2. NACA Subcommittee on Lubrication and Wear: Review of Current and Anticipated Lubricant Problems in Turbojet Engines. NACA RM 51D20, 1951.

3. Perlmutter, Isaac: Rolling Contact Bearings for High Temperature Applications. Memo. Rep. WCRTL-M-5620, Materials Lab., Res. Div., Wright-Patterson Air Force Base, Dayton (Ohio), Apr. 15, 1952.

4. SAE Panel on High-Speed Rolling-Contact Bearings: Trends of Rolling-Contact Bearings as Applied to Aircraft Gas-Turbine Engines. NACA TN 3110, 1954.

5. Barnes, Gilbert C., and Ryder, Earle A.: A Look at Some Turbine Bearing Problems. Preprint No. 693, SAE, 1956.

6. Jones, A. B.: New Departure - Analysis of Stresses and Deflections. Vols. I and II. New Departure, Div. General Motors Corp., Bristol (Conn.), 1946.

7. Lundberg, G., and Palmgren, A.: Dynamic Capacity of Rolling Bearings. ACTA Polytech., Mech. Eng. Ser., vol. 1, no. 3, 1947.

8. Bear, H. Robert, and Butler, Robert H.: Preliminary Metallographic Studies of Ball Fatigue Under Rolling-Contact Conditions. NACA TN 3925, 1956.

9. Macks, E. F.: The Fatigue Spin Rig - A New Apparatus for Rapidly Evaluating Materials and Lubricants for Rolling Contact. Lubrication Eng., vol. 9, no. 5, Oct. 1953, pp. 254-258.

10. Johnson, Leonard G.: The Median Ranks of Sample Values in Their Population with an Application to Certain Fatigue Studies. Ind. Math., vol. 2, 1951, pp. 1-9.

11. Anon.: SAE Handbook. Soc. Automotive Engs., Inc. (New York), 1950, p. 286.

TABLE I. - ANALYSIS OF TEST STEELS

Steel	Composition, percent								
	C	Si	Mn	P_{max}	S_{max}	Cr	W	Mo	V
SAE 52100[a]	0.95 to 1.10	0.20 to 0.35	0.25 to 0.45	0.025	0.025	1.30 to 1.60	----	----	----
AISI M-1[b]	0.80	0.30	0.25	-----	-----	4.00	1.50	8.50	1.00
AISI M-50 (MV-1)[b,c]	0.80	0.25	0.30	-----	-----	4.10	----	4.25	1.10

[a]Ref. 11.

[b]Manufacturer's data.

[c]Cylinders only.

TABLE II. - TEST CONDITIONS

Steel	Number of balls tested	Ball diameter, in.	Track orientation (a)	Maximum Hertz stress applied, psi	Approximate rate of stressing, cycles/hr	Average ball weight, grams	Lubricant
AISI M-1	21	0.500	Coincident with equator	720,000	11.3×10^6	8.3647	Sebacate and additives
SAE 52100	21	.500	Coincident with equator	714,000	11.4	8.2002	Sebacate and additives
SAE 52100	13	.500	Across poles	714,000	11.4	8.2022	Sebacate and additives
SAE 52100	50	.5625	Random	600,000	7.3	11.827	Mineral oil (SAE 10)
SAE 52100	50	.5625	Random	675,000	8.7	11.827	Mineral oil (SAE 10)
SAE 52100	50	.5625	Random	750,000	10.0	11.827	Mineral oil (SAE 10)

[a]See text and figs. 9, 10, and 12.

TABLE III. - DISTRIBUTION OF FAILURES IN BALLS

ORIENTED TO RUN DIRECTLY OVER POLE

[1/2-In. SAE 52100 balls; pole half-angle, 38°.]

Location of failures	Experimental results		Theoretical fraction of failures,[a] percent	Ratio of experimental to theoretical results
	Number of failures	Fraction of failures, percent		
Polar area	12	92	42.2	2.17
Outside polar area	1	8	57.8	.14

[a]For a homogeneous material.

TABLE IV. - EXPERIMENTAL AND THEORETICAL

DISTRIBUTIONS OF TRACK ORIENTATION

[Random orientation; 150 balls; pole half-angle, 40°.]

Track location	Experimental results		Theoretical fraction of tracks, percent
	Number of tracks	Fraction of tracks, percent	
Through polar areas	85	56.7 [a]62.4	64
Polar boundary	17	11.3	--
Entirely out of polar areas	48	32 [a]37.6	36

[a]Value includes one-half of polar boundary tracks.

TABLE V. - EXPERIMENTAL AND THEORETICAL FAILURE

LOCATION DISTRIBUTIONS FOR ALL FAILURES IN

RANDOMLY ORIENTED BALLS

[9/16-In. SAE 52100 balls; pole half-angle, 40°.]

Location of failures	Experimental results		Theoretical fraction of failures,[a] percent	Ratio of experimental to theoretical results
	Number of failures	Fraction of failures, percent		
Polar areas	7	24.1 } [b]29.3	15.3	1.92
Polar-area boundary	3	10.3	----	----
Outside polar areas	19	65.6 } [b]70.7	84.7	.83

[a]For a homogeneous material.

[b]This value includes one-half of polar boundary failures.

TABLE VI. - DISTRIBUTION OF FAILURES IN RANDOMLY

ORIENTED BALLS WHICH RAN OVER POLES

[9/16-In. SAE 52100 balls; pole half-angle, 40°.]

Location of failures	Experimental results		Theoretical fraction of failures,[a] percent	Ratio of experimental to theoretical results
	Number of failures	Fraction of failures, percent		
Polar areas	7	44	23.4	1.88
Outside polar areas	9	56	76.6	.73

[a]For a homogeneous material.

TABLE VII. - SUMMARY OF FAILURE LOCATION AND CAUSE

[9/16-In. SAE 52100 balls with randomly oriented tracks.]

Converted life, cycles (a)	Maximum Hertz stress, psi	Failure latitude, deg	Failure location	Failure cause
5.5×10^6	750×10^3	88	Polar	Unknown
6.89	600	82	Polar	Unknown
12.1	600	60	Nonpolar	Inclusion perpendicular to equator (fig. 5(b))
12.3	750	9	Nonpolar	Inclusion perpendicular to equator (fig. 5(d))
17.9	750	63	Polar boundary	Unknown
20.0	750	9	Nonpolar	Inclusion perpendicular to equator (fig. 5(a))
40.5	675	6	Nonpolar	Inclusion perpendicular to equator (fig. 5(c))
80.8	600	7	Nonpolar	Large prerun corrosion pit on track
203	600	34	Nonpolar	Prerun corrosion pit on track
204	600	55	Polar	Unknown
221	675	83	Polar	Unknown
336	675	38	Nonpolar	Unknown
358	675	57	Polar boundary	Inclusion perpendicular to equator
384	600	43	Nonpolar	Inclusion perpendicular to equator 15° to track
399	600	72	Polar	Unknown
418	675	33	Nonpolar	Inclusion perpendicular to equator
458	675	21	Nonpolar	Unknown
486	750	36	Polar boundary	Crack perpendicular to equator
712	750	57	Polar boundary	Unknown
756	675	35	Nonpolar	Unknown
841	750	79	Polar	Unknown
946	675	79	Polar	Unknown
948	750	21	Nonpolar	Unknown
988	675	34	Nonpolar	Unknown
1155	750	19	Nonpolar	Unknown
1300	750	4	Nonpolar	Unknown
1606	750	21	Nonpolar	Unknown
1665	750	12	Nonpolar	Unknown
2184	750	0	Equator	Unknown

aEquivalent life at 675,000 psi Hertz stress.

(a) Cutaway view.

(b) Schematic diagram

Figure 1. - Rolling-contact fatigue spin rig.

4271

(a) SAE 52100 balls
    run across poles.
    Maximum Hertz
    stress, 714,000
    psi.

(b) SAE 52100 balls run
    on equator. Maximum
    Hertz stress, 714,000
    psi.

(c) AISI M-1 balls run
    on equator. Maximum
    Hertz stress, 720,000
    psi.
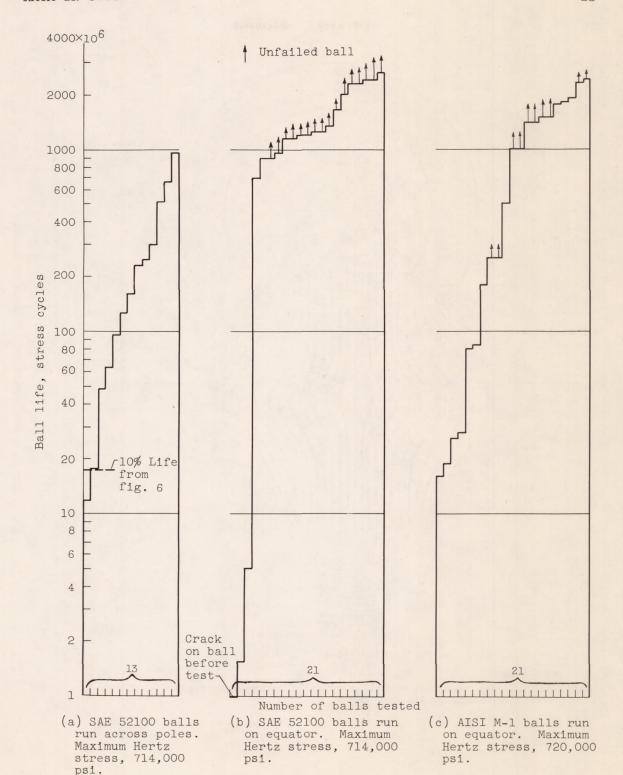
Figure 2. - Comparison of tests in which balls ran on equator and across
    poles. Room temperature; 1/2-inch balls with 0.050-inch hole drilled
    through; lubricant flow rate, 5 milliliters per hour; lubricant,
    synthetic sebacate.
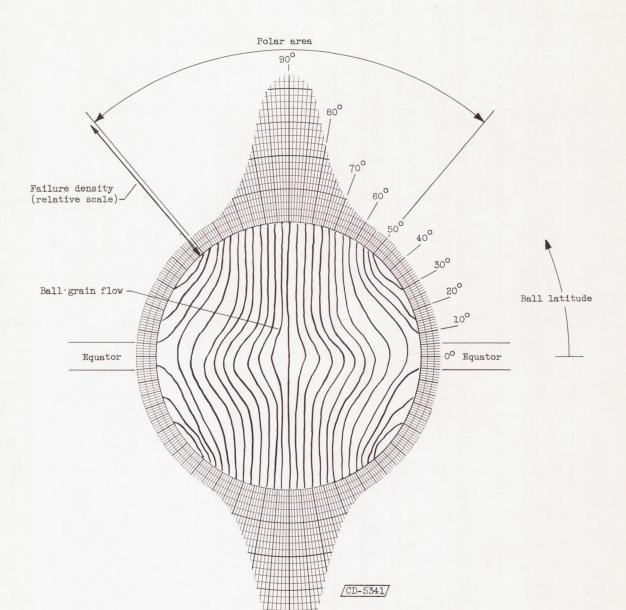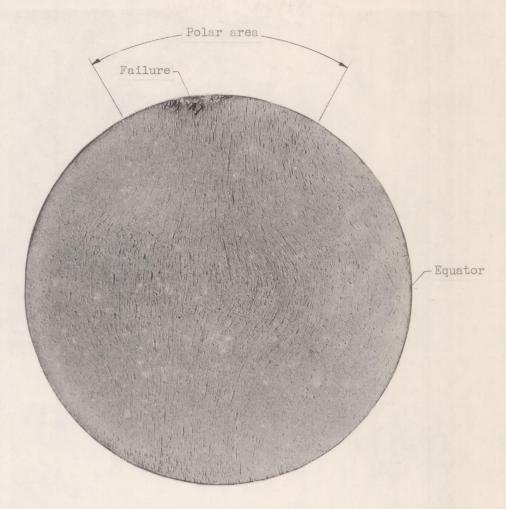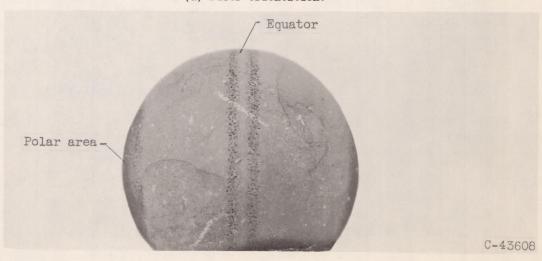
Figure 3. - Failure density plotted against ball latitude with cross section showing
    grain flow. 9/16-Inch SAE 52100 balls.
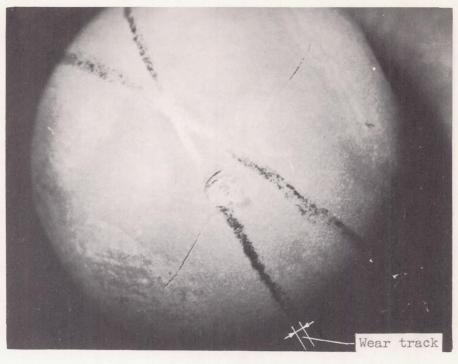
(a) Fiber orientation.
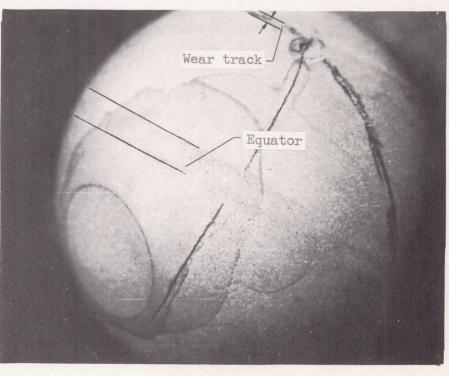
(b) Poles and equator.

Figure 4. - Fiber orientation on SAE 52100 balls (macroetched).

(a)

(b)
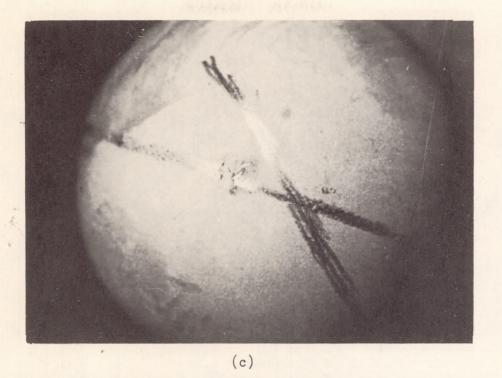
C-43605

Figure 5. - Typical failure-causing inclusions perpendicular to equator
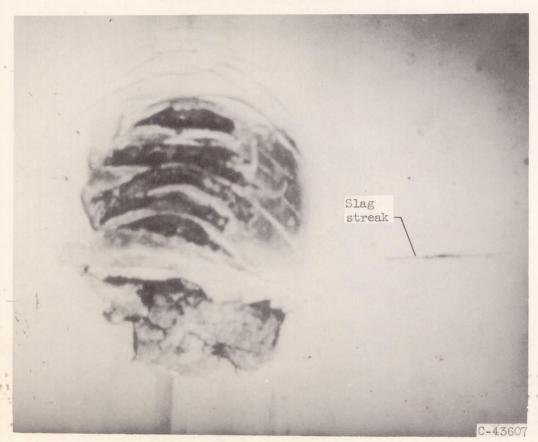and coincident with failure fault line.

CK-4 back

(c)

(d)   C-43604
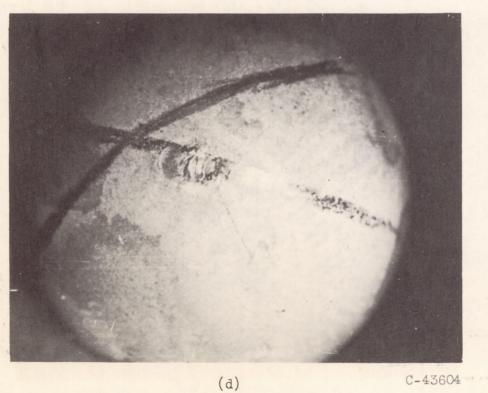
Figure 5. - Concluded. Typical failure-causing inclusions perpendicular
to equator and coincident with failure fault line.
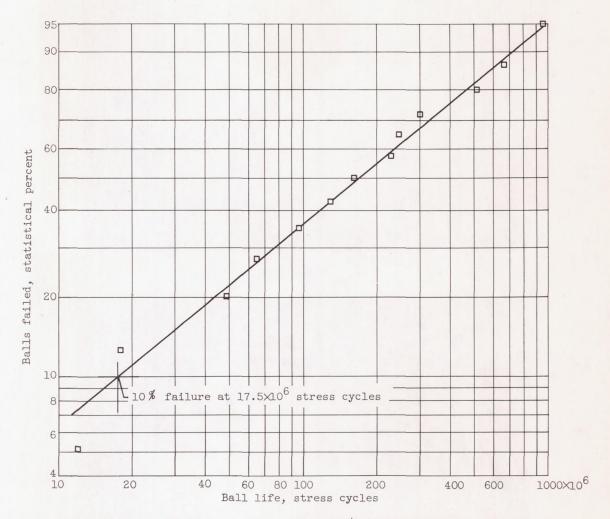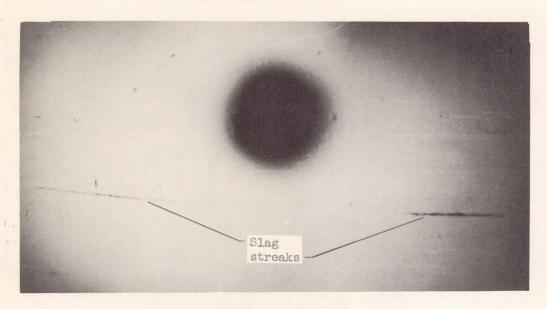
Figure 6. - Weibull plot of stress life of 1/2-inch SAE 52100 balls run over
  poles. Maximum Hertz stress, 714,000 psi; room temperature; lubricant
  flow rate, 5 milliliters per hour; lubricant, synthetic sebacate.

4271
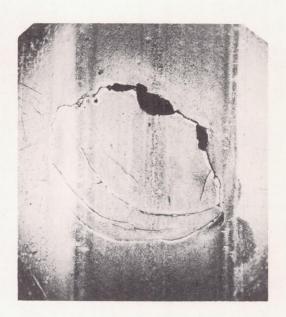
(a) Representative slag streaks.

(b) Failure originating at slag streak.

Figure 7. - Slag streaks on AISI M-1 balls.

(a) Ball track fatigue
    failure, before spalling.

(b) Ball track fatigue
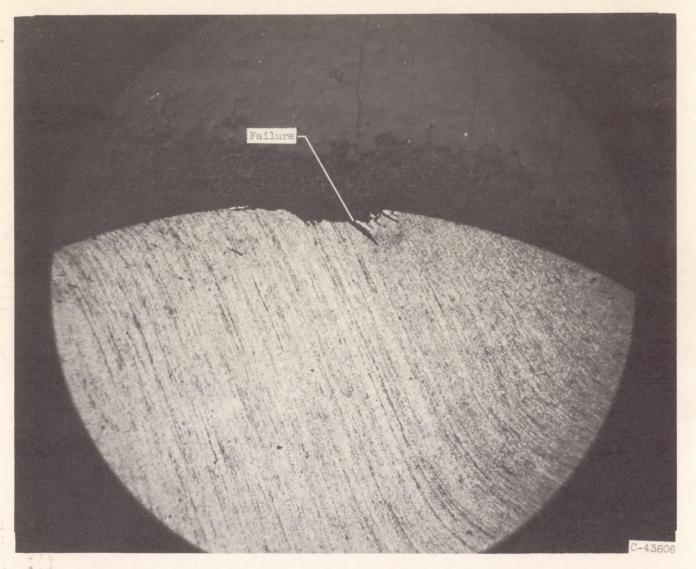   failure, after spalling.

Figure 8. - Degree of spalling (ref. 8).

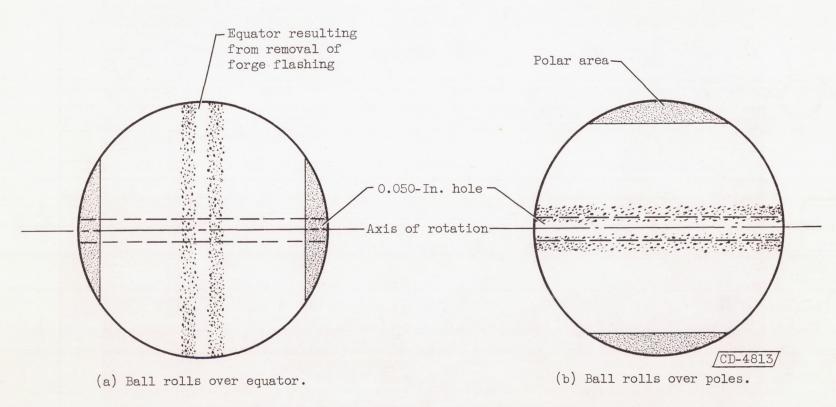Figure 9. - Pole failure on SAE 52100 ball (sectioned and macroetched).

Equator resulting
from removal of
forge flashing

Polar area

0.050-In. hole

Axis of rotation

CD-4813

(a) Ball rolls over equator.

(b) Ball rolls over poles.

Figure 10. - Schematic drawing of test balls lightly etched to show relation of axis -
determining hole to forging direction.

35-Mm camera
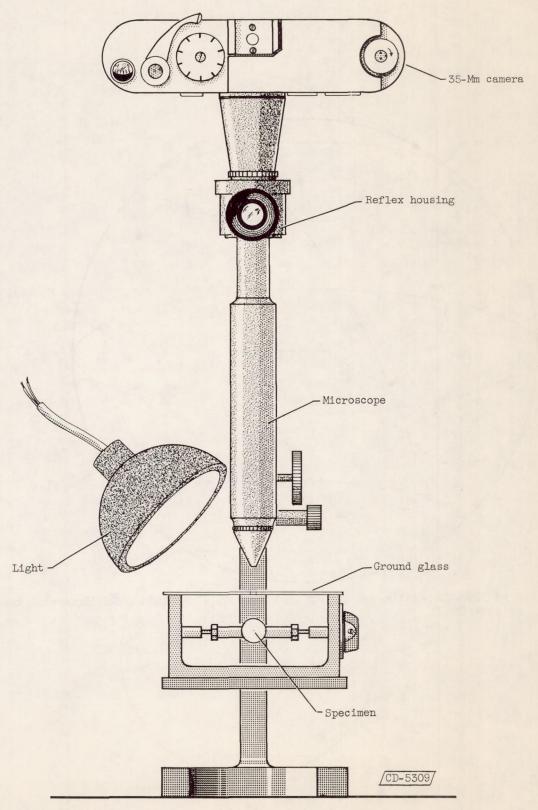
Reflex housing

Microscope

Light

Ground glass

Specimen

CD-5309

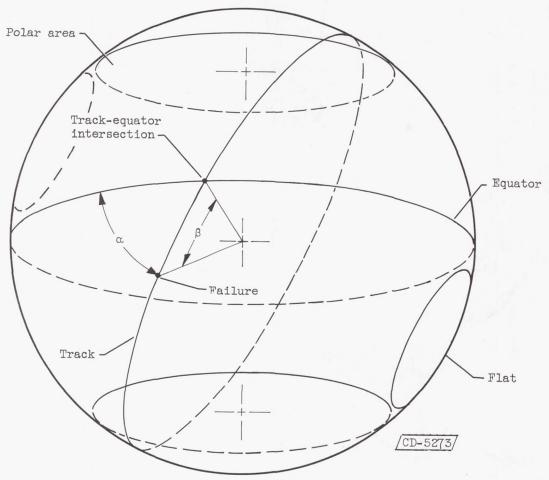Figure 11. - Photographic apparatus.

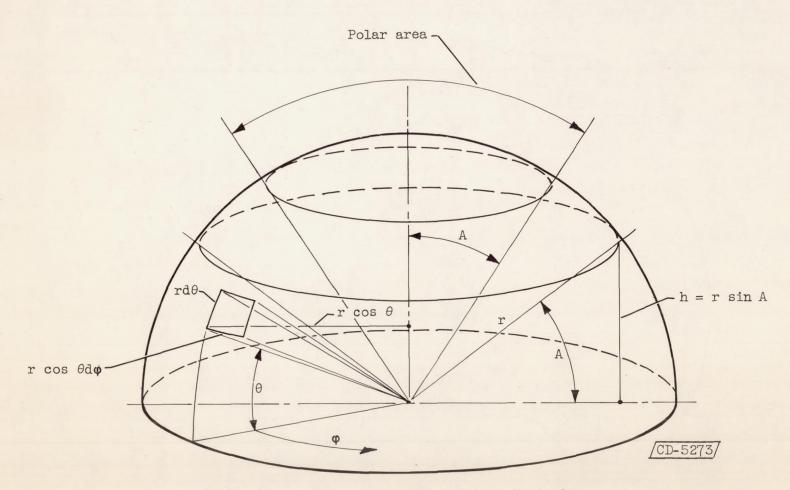Figure 12. - Schematic drawing of test ball showing flats which determine track orientation.

Figure 13. - Schematic drawing of ball hemisphere.